

# Study on HIC and SSC of the Electric Resistance Welded Linepipe Steel

† Wan Keun Kim<sup>1</sup>, Seong Ung Koh<sup>2</sup>, Boo Young Yang<sup>2</sup>, and Kyoo Young Kim<sup>1</sup>

<sup>1</sup>Dept. of Mat. Sci. and Eng., Pohang Univ. of Sci. and Tech.,  
San 31, Hyoja-Dong, Nam-gu, Pohang 790-784 Korea

<sup>2</sup>Technical Research Center, POSCO,  
Geidong-Dong, Nam-gu, Pohang 790-704 Korea

The resistance of the linepipe steel to hydrogen-induced cracking (HIC) and sulfide stress cracking (SSC) is very important for steel to be used in sour oil/gas environments. Welding of steels is necessary to the construction of pipe-line transporting oil/gas. In this study, HIC and SSC resistance of an electric resistance welded (ERW) steel plate which belongs to API X70 grade was evaluated by using NACE TM0284-96A and NACE TM0177-96A methods. HIC and SSC fracturing behavior was investigated by observing fractured surfaces using optical microscopy (OM) and scanning electron microscopy (SEM). It was discussed in terms of metallurgical parameters such as the distribution of primary microstructure, second phases and inclusions. Results showed that the weld joint of ERW steel is more sensitive than base metal to HIC and SSC. This is due to difference in the contribution of metallurgical parameters to HIC and SSC nucleation and propagation.

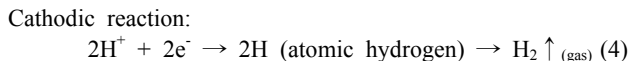
**Keywords** : ERW, HIC, SSC, diffusible hydrogen, metallurgical factor.

## 1. Introduction

Cracking that line pipe steels may encounter in sour environments containing hydrogen sulfide gas (H<sub>2</sub>S) is generally categorized into two types; HIC and SSC. HIC is a kind of the hydrogen embrittlement which occurs in the form of surface blisters and/or internal cracks in the absence of applied stress. HIC is commonly found in steels with high impurity levels that have a high density of large planar inclusions and/or regions of anomalous microstructure produced by segregation of impurity and alloying elements in the steel. In steels, the development of internal cracks tends to link with other cracks. The link-up of these cracks on different planes in steels is often referred to as stepwise cracking.<sup>1)</sup> On the other hand, SSC occurs under externally or internally stressed or strained conditions and propagates perpendicularly to the tensile stress direction. SSC of line pipe steels exposed to sour media under stress is classified into two types; type I and type II. Type I SSC can be understood in two stages. The initial stage of cracking is the process of hydrogen induced cracking which is characterized by cracks parallel to applied stress. In the latter stage, the cracks link together perpen-

dicular to applied stress. Type I SSC is referred to as stress oriented hydrogen induced cracking (SOHIC) rather than SSC.<sup>2)</sup> However, Type II SSC is recognized as the typical cracking resulted from hydrogen embrittlement. The failure occurs in the way of quasi-cleavage, and as a consequence, the cracking propagates in the direction perpendicular to applied stress. It has been reported that specifying the maximum hardness of 248 in Vickers hardness may prevent the incidence due to type II SSC.<sup>2-4)</sup>

Both HIC and SSC belong to hydrogen embrittlement developed by sulfide corrosion process on the steel surface in the presence of hydrogen sulfide. The most accepted corrosion reactions of steel exposed to a sour gas are:



Reaction (2) represents the first dissociation of H<sub>2</sub>S,

† Corresponding author: kwk@postech.ac.kr

whiled reaction (3) does the second dissociation to produce two ions of hydrogen. These ions produced at the cathode combine with electrons released by the steel to form atomic hydrogen at the steel surface. The hydrogen atoms form gaseous hydrogen; however, the presence of hydrogen sulfide ions ( $\text{HS}^-$ ) reduces the rate of hydrogen gas formation. Thus, some atomic hydrogen diffuses into the steel. As hydrogen diffuses, it encounters trapping sites and is collected there, forming hydrogen gas at very high pressures. The hydrogen trapping sites presented are metallurgical defects, such as non metallic inclusions, large precipitates, and bands of hard microstructures. A common feature of these sites is that they are planar and oriented in the direction parallel to the pipe wall. As hydrogen is collected at the trapping sites, the high pressure developed causes a stress concentration at the edge of the site, disbanding the interface and forming a crack.<sup>5)</sup>

Welding of steels in the construction of pipe-line transporting oil/gas is necessary. However, HAZ regions in the welded steels have high susceptibility to hydrogen embrittlement in both service and laboratory environments.<sup>4)</sup> The objective of this paper is to investigate the difference in HIC and SSC characteristics of electric resistance welded line pipe steels and to clarify the effect of metallurgical factors on both HIC and SSC.

## 2. Experimental procedure

### 2.1 Microstructure and mechanical properties

An electric resistance welded (ERW) steel plate which belongs to API X70grade with thickness of 13 mm was used as specimen. The ERW steel plate basically includes 0.05%C and 0.25%Cr. The specimens composed of base metal and weld joint were ground up to #2,000 with silicon carbide (SiC) paper and polished with 1 $\mu\text{m}$  diamond suspension. For microstructure observation, the specimens were then degreased with acetone and etched with a nital solution (a mixture of 5% nitric acid and ethanol). The microstructure was examined with optical microscope (OM) and a scanning electron microscope (SEM).

The yield strength (YS) and ultimate tensile strength (UTS) of two steels were determined by using a tensile testing machine. The hardness values were measured by micro and ultra-micro Vicker's hardness tester.

### 2.2 HIC and SSC tests

HIC and SSC tests were performed respectively in reference to NACE TM0284-96 and NACE TM0177-96A standard test method in a solution saturated with  $\text{H}_2\text{S}$  gas, including 5 wt% NaCl and 0.5 wt%  $\text{CH}_3\text{COOH}$  dissolved in distilled water. In particular, SSC tests were conducted

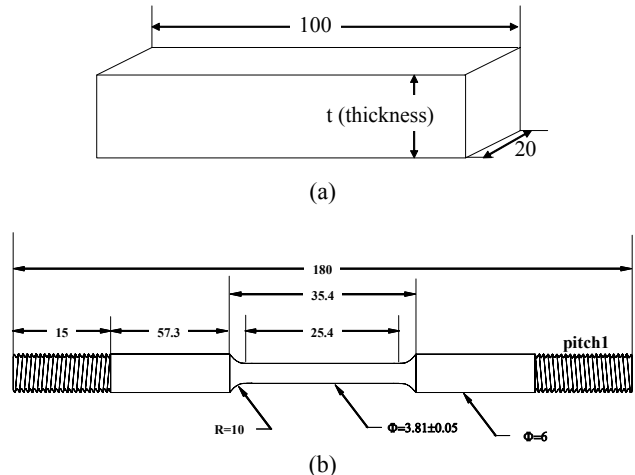


Fig. 1. Schematic of specimen for HIC and SSC tests; (a) HIC, (b) SSC

by constant load test (CLT). Fig. 1 shows schematic of specimens for HIC and SSC tests.<sup>6,7)</sup> After testing, HIC sensitivity was measured in terms of crack area ratio (CAR) by using ultrasonic detector, while SSC sensitivity was measured in terms of threshold stress meaning maximum load fraction for yield strength (YS) of steels which was not fractured for 720 hrs.

### 2.3 Inclusion and fractography analysis

To elucidate the effect of inclusions on HIC of steels, the relative amount, size and distribution of inclusions in two steels were investigated using OM and SEM. To determine the chemical composition of inclusions in steels, energy dispersive spectroscopy (EDS) was used. After HIC testing, fracture behavior was analyzed using OM and SEM in order to examine crack initiation sites and propagation path.

## 3. Results and discussion

### 3.1 Microstructure, mechanical properties and inclusion

Microstructure is classified into two parts, base metal and weld joint as shown in Fig. 2. The size of weld joint is about 20 mm, while that of heat affected zone (HAZ) is about 2-3mm. In contrast to typical arc welding, electric resistance welding is performed without welding metal. This causes decrease in weld size and probability of defect formation. HAZ includes coarse grain region (C.G) and fine grain region from the center of partially molten zone, bonding line. Each zone is characterized by a specific temperature interval;  $1100 < \text{C.G} < 1450$  °C,  $\text{AC3} < \text{F.G} < 1100$  °C.<sup>4)</sup>

Fig. 2 shows microstructure of base metal and weld joint. Basically, base metal includes ferrite (F), acicular

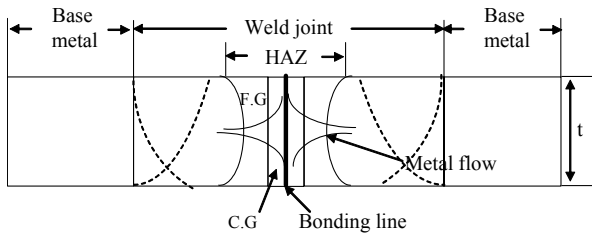


Fig. 2. Schematic showing microstructures of base metal and weld joint

ferrite (AF) and bainitic ferrite (BF) as shown in Fig. 3 (a). BF was defined as second phase including a lot of carbide particles and having hardness of over 260 Hv. Also, base metal includes martensite austenite (M/A) having hardness over 300 Hv. However, the microstructure of HAZ is composed of the typical F and pearlite (P) as presented in Fig. 3(b). The grain size of C.G HAZ is larger than that of F.G HAZ. The characteristics of microstructure determine yield strength (YS) and hardness value of base metal and weld joint as listed in Table 1. That is, both yield strength and hardness value of base metal containing BF is higher than those of weld joint, and hardness value of F.G HAZ is higher than that of C.G HAZ.

On the other hand, most of inclusions in base metal and weld joint are non spherical oxide inclusions. As

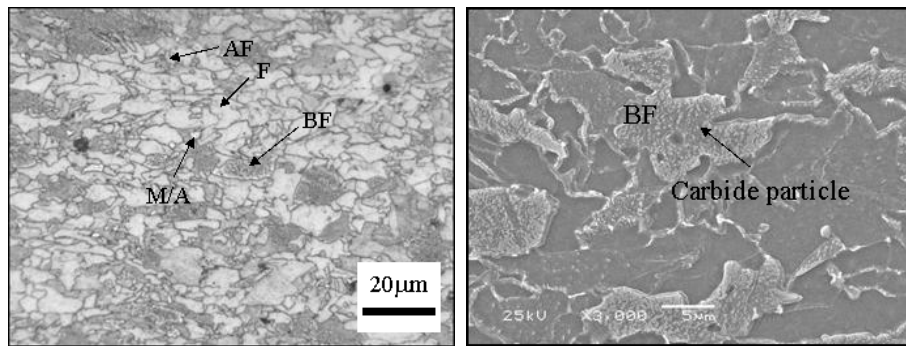
Table 1. Yield strength and hardness values of base metal and weld joint

Steel	Base metal	Weld joint	
Yield strength (kg/mm <sup>2</sup> )	57.5	48.8	
Hardness (Hv)		C.G HAZ	F.G HAZ
Denting load: 100gf		208	218

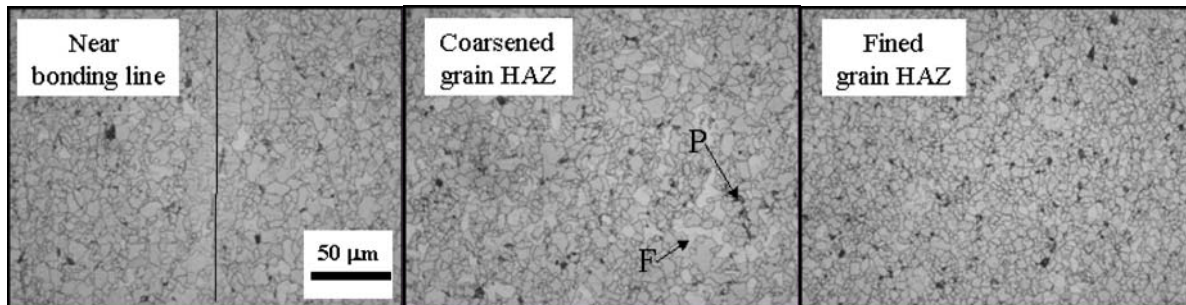
shown in Fig. 4, an inclusion in base metal include primarily Al, Ca, Mg and O, while that in bonding line of weld joint does Fe, Mn, Si, O. In case of base metal, the maximum size of a single inclusion was 50 m and the inclusion cluster with size over hundreds of micro-meters was observed at thickness over 4 position as well as single inclusions. Although inclusions including Al, Ca, Mg and O were observed in weld joint, most of inclusions nearby bonding line include Fe, Mn, Si, O. The inclusions are due to re-oxidation in the molten center of weld joint under welding process.

### 3.2 HIC and SSC resistance

After HIC tests, cracking sensitivity was measured in terms of CAR by an ultrasonic detector. As shown in Table 2, HIC occurred in all of base metal and weld joint, and crack area ratio (CAR) of base metal is lower than that

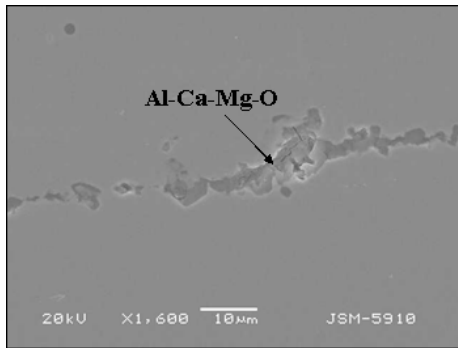


(a)

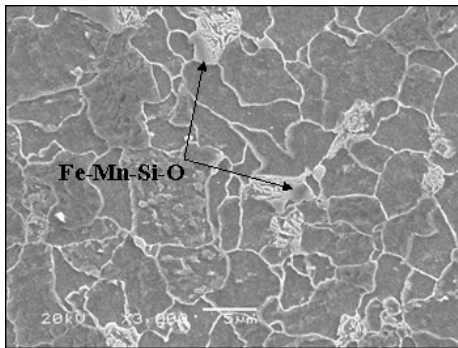


(b)

Fig. 3. Microstructure of base metal and weld joint; (a) Base metal, (b) Weld joint



(a)



(b)

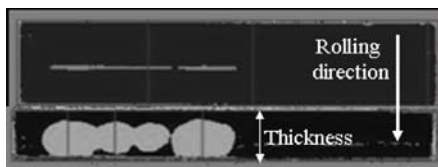
Fig. 4. Species of inclusion in base metal and nearby bonding line of weld joint; (a) Base metal, (b) Bonding line of weld joint

Table 2. HIC and SSC resistance of base metal and weld joint

Steel	Base metal	Weld joint
CAR (%)	5.45	22.5
Threshold stress (YS%)	78	Less than 70



(a)



(b)

Fig. 5. Ultrasonic detection results after HIC tests; (a) Base metal (b) Weld joint

of weld joint. This means that weld joint is more sensitive to HIC than base metal. As presented in Fig. 5, in case

of base metal, HIC occurred at t/4 position in the form of blisters and propagated in direction parallel to rolling plane. However, in contrast to base metal, HIC in weld joint was initiated around bonding line of weld joint regardless of thickness of steel and propagated in direction perpendicular to rolling plane. Also, it can be confirmed that SSC resistance of base metal is higher than that of weld joint in similar to HIC sensitivity from Table 2. Threshold stress of base metal is 78%YS while weld joint was fractured even under load less than 70%YS.

### 3.3 Crack nucleation and propagation

HIC of base metal nucleated at a single inclusion and/or at a cluster of oxide-inclusions including Al, Ca, Mg and oxide. Figs. 6(a), 6(b) and 6(c) show the HIC fracture surface which reveals typical crack initiation at an oxide cluster and a single inclusion in base metal. The valley aligned in Fig. 6(a) resulted from inter-connection of a few nucleation sites, as shown in magnified view in Fig. 6(b). As soon as HIC occurs at an oxide cluster, cracks propagated in the quasi-cleavage manner. However, in case of HIC nucleation at single oxide inclusion, micro-dimples with size of about 1 µm were observed on every side of HIC nucleation sites as shown in Fig. 6(d). This means that micro-dimples from oxides acting as nucleation sites propagate to critical crack size for quasi-cleavage crack advance. Fig. 6(e) is a cross-section obtained by cutting a line shown in Fig. 6(a), and it implies that BF contributes to form micro-dimples for quasi-cleavage crack advance. But, the clear reason for micro-dimple formation will not be discussed in this paper. A single inclusion and/or a cluster of oxide-inclusions, which acts as crack nucleation site in the steel including F, AF and BF as primary phases, are about 20 µm in maximum length. Cracks propagated in quasi-cleavage manner following the hard second phases such as M/A as presented in Fig. 6(f).

Unlike HIC fracture surface of base metal, that of weld joint is very flat and coherent as shown in Figs. 7(a), 7(b), and 7(c). HIC in weld joint was initiated at a lot of inclusions including Fe-Mn-Si oxide. As soon as HIC nucleates at oxide inclusions, cracks propagated in the quasi-cleavage manner without formation of micro-dimples. As presented in Fig. 7(b), this phenomenon is expected to be due to a lot of inclusions acting as irreversible trap sites on the fracture surface. Fig. 7(d) shows a cross-section of a crack and represents HIC nucleation and propagation around bonding line. HIC in weld joint propagated following the boundaries between grains nearby bonding line and coarsened grains by the significant decrease in hardness value around bonding line as shown in Figs. 7(e) and 7(f).

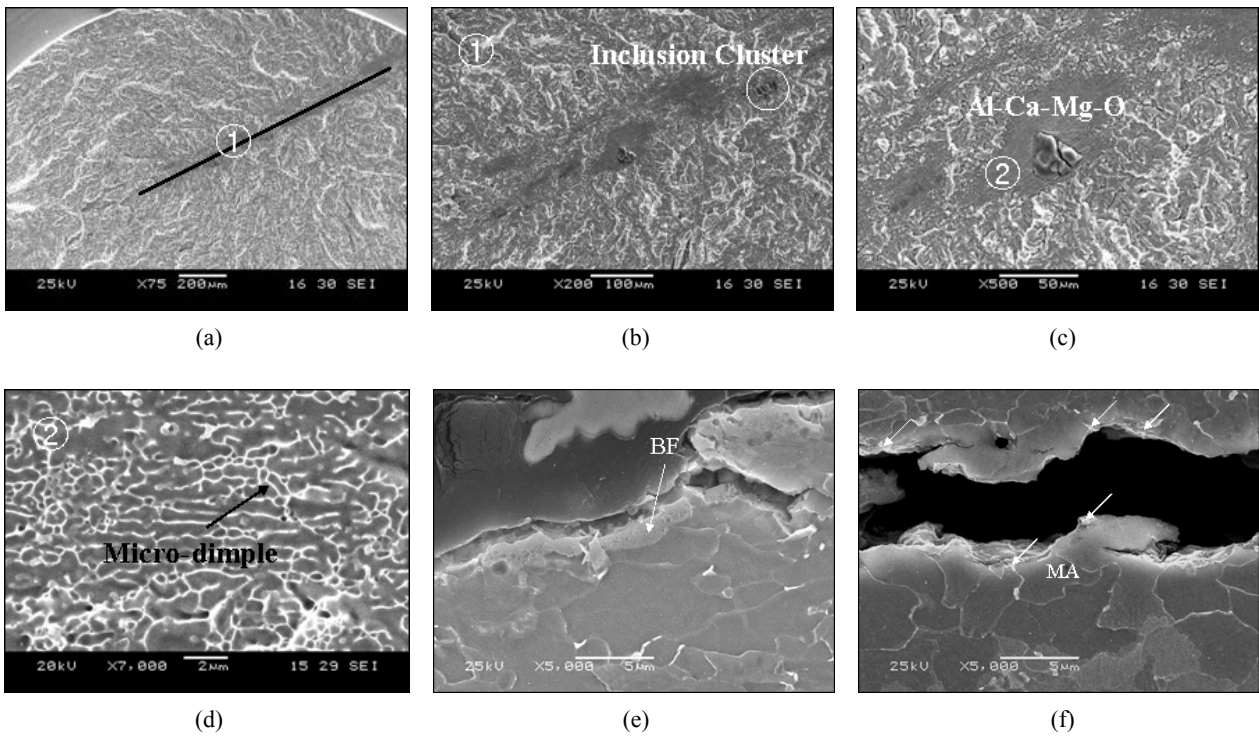


**Fig. 6.** HIC nucleation and propagation of base metal; (a) Fracture surface, (b) and (c) HIC nucleation at a single inclusion and/or at a cluster of oxide-inclusions, (d) The formation of micro-dimples, (e) and (f) HIC propagation path

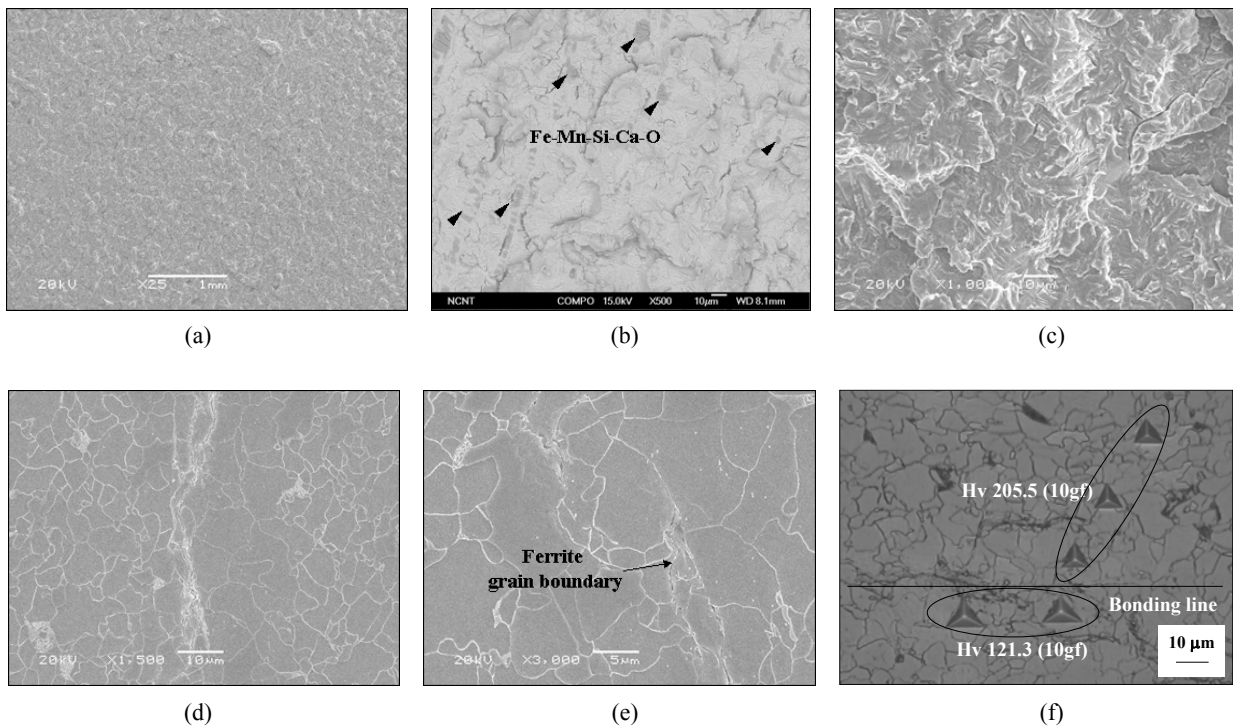


**Fig. 7.** HIC nucleation and propagation of weld joint; (a) Fracture surface, (b) HIC nucleation at a lot of oxide-inclusions, (c) HIC propagation in quasi-cleavage manner, (d), (e) and (f) HIC propagation path

On the other hand, after SSC tests, base metal was fractured in types of SOHIC as shown in Fig. 8. Base metal was fractured by connection of a few small cracks perpendicular to loading axis formed in terms of stress concentration after bending of SOHIC. After SSC testing with increasing test time, it was confirmed that SOHIC cracks are connected by cracks perpendicular to tensile axis. Fig. 8(a), 8(b) and 8(c) show nucleation sites of the cracks perpendicular to tensile axis on the fracture surface. The cracks nucleated at a single inclusion with size over 10  $\mu\text{m}$  and propagated in quasi-cleavage manner. Also, Fig. 8(d) represents a crack of typical SOHIC mode and Fig. 8(e) shows SOHIC nucleation at an oxide cluster and single oxide inclusion. Fracture surfaces of SOHIC and HIC are similar to each other. However, failure by SOHIC mode does not accompany formation of micro-dimples.

In contrast to fracture mode of base metal, weld joint was fractured in SSC type II mode by hydrogen embrittlement. As shown in Figs. 9(a) and 9(b), as soon as nucleating, cracks perpendicular to tensile axis propagated in the quasi-cleavage manner without formation of SOHIC. Also, Figs. 9(c), 9(d) and 9(e) show that the cracks nucleated at oxide inclusions including Fe-Mn-Si-Ca oxide and propagated following ferrite grain boundaries nearby bonding line like HIC of weld joint.

To improve HIC and SSC resistance of steels, various technologies such as addition of proper alloying elements, high cleanliness and Ca treatment during steel making processes are required. But, microstructure control of steels is basically more important than those mentioned earlier.<sup>8)</sup> For HIC and SSC resistant steels, the formation of BF and MA sensitive to hydrogen embrittlement should be restrained in thermo-mechanical controlled process (TMCP) and the significant decrease of hardness around bonding line of weld joint should be reduced. Also, large inclusions such as elongated manganese sulfides and clusters or stringers of oxides increase the HIC and SSC susceptibility of steels.<sup>9),10)</sup> Considering HIC and SSC nucleation at a single inclusion and/or at a cluster of oxide inclusions, Ca treatment is necessary to control the shape of such inclusions in steel making process. In particular, to improve HIC and SSC resistance of weld joint, re-oxidation in the molten center of it should be restrained under ERW process.

#### 4. Conclusions

In this paper, HIC and SSC resistance of an electric resistance welded steel plate which belongs to API X70 grade was evaluated and the effect of metallurgical factors

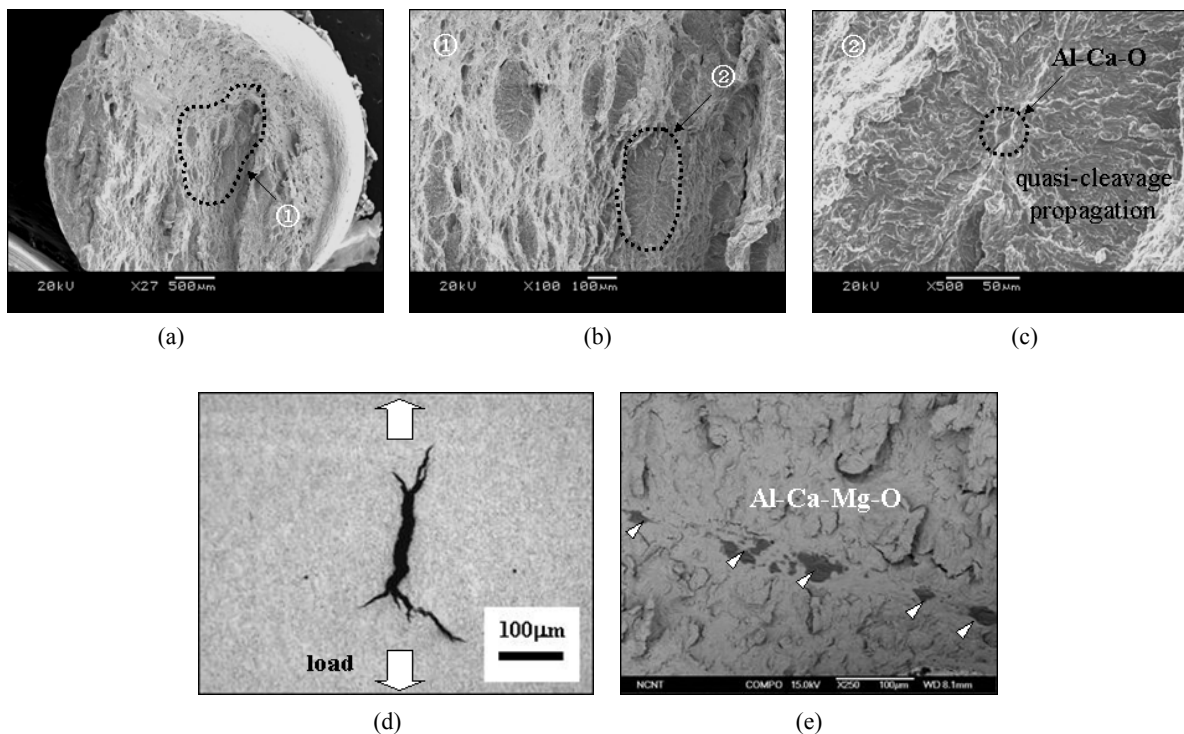


**Fig. 8.** SSC nucleation and propagation of base metal; (a) Fracture surface, (b) and (c) Nucleation of cracks perpendicular to load axis, (d) A cross-section showing typical SOHIC, (e) SOHIC nucleation at an oxide cluster and single oxide inclusion

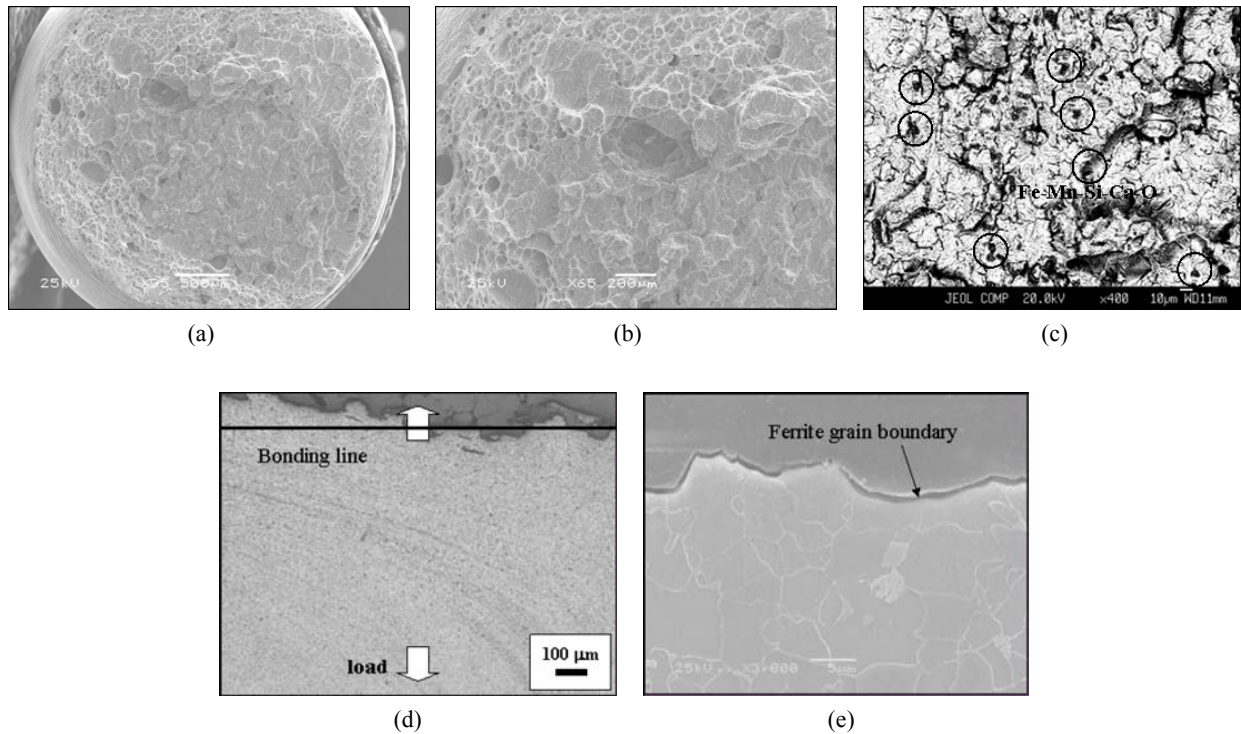


**Fig. 9.** SSC nucleation and propagation of weld joint; (a) and (b) Fracture surface, (c) Nucleation of cracks perpendicular to load axis, (d) A cross-section showing failure around bonding line, (e) SSC propagation following ferrite grain boundaries

on HIC and SSC nucleation and propagation of base metal and weld joint was investigated.

1) For steel including F, AF and BF, after HIC nucleation at single oxide inclusion, micro-dimples with size of about  $1\ \mu\text{m}$  is observed on every side of HIC nucleation sites. The micro-dimples from nucleation sites propagate to critical crack size for quasi-cleavage crack advance.

2) For HIC and SSC resistant steels, the formation of BF and MA sensitive to hydrogen embrittlement should be restrained in thermo-mechanical controlled process (TMCP) and the significant decrease in hardness around bonding line of weld joint should be reduced.

3) In case of SOHIC fracture mode, steels are fractured by connection of a few small cracks perpendicular to loading axis, formed by stress concentration after bending of SOHIC

4) To improve HIC and SSC resistance of weld joint, re-oxidation in the molten center of it should be restrained under ERW process.

## References

1. NACE committee, *Review of published literature on wet H<sub>2</sub>S cracking of steels through 1989* (2003).
2. M.kimura, *CORROSION*, **44**, 738 (1998).
3. J. L. Albarran, A. Aguilar, L. Martinez, and H.F.Lopez, *CORROSION*, **58**, 783 (2002).
4. G. M. Omweg, G. S. Frankel, W. A. Bruce, J. E. Ramirez, and G. Koch, *CORROSION*, **59**, 640 (2003).
5. J. L. Gonzalez, R. Ramirez, J. M. Hallen, and R. A. Guzman, *CORROSION*, **53**, 935 (1997).
6. NACE standard TM0284-96, *Evaluation of pipeline and pressure vessel steels for resistance to hydrogen-induced cracking* (1996).
7. NACE standard TM0177-96, *Evaluation of pipeline and pressure vessel steels for resistance to sulfide stress cracking* (1996).
8. R. A. Caneiro, R. C. Ratnapuli, and V. F. C. Lins, *Materials Science and Engineering A*, **357**, 104 (2003).
9. G. Domizzi, G. Anteri, J.OVEJERO-Garcia, *Corrosion Science*, **43**, 325 (2001).
10. T. Hara, H. Asahi, and H. Ogawa, *CORROSION*, **60**, 1113 (2004).